HHS Public Access

Author manuscript

Metabolism. Author manuscript; available in PMC 2026 April 03.

Published in final edited form as:

Metabolism. 2026 January ; 174: 156427. doi:10.1016/j.metabol.2025.156427.

Hepatic steatosis associates with leukopoietic activity and atherosclerotic inflammation: mechanistic insights into cardiovascular risk☆

Shady Abohashem[a,h,*], **Wesam Aldosoky**[a], **Taimur Abbasi**[b], **Tawseef Dar**[c], **Robert Rollings**[a], **Brian Tung**[d], **Basma Hammad**[e], **Fatima Saeed**[a], **Abdelrahman Ali**[f], **Richard A.P. Takx**[g], **Brian B. Ghoshhajra**[a], **Ahmed Tawakol**[a,h], **Michael T. Osborne**[a,h]

[a]Cardiovascular Imaging Research Center, Radiology Department, Massachusetts General Hospital, Harvard Medical School, Boston, USA

[b]Department of Internal Medicine, Rush University Medical Center, Chicago, USA

[c]Cardiology Department, Mount Sinai Medical Center, NYC, USA

[d]Radiology Department, Westchester Medical Center, NYC, USA

[e]Cardiology Department, Alexandria University, Alexandria, Egypt

[f]Cardio-oncology Department, MD Anderson Cancer Center, Houston, USA

[g]Radiology Department, Amsterdam University Medical Center, Amsterdam, Netherlands

[h]Cardiology Department, Massachusetts General Hospital, Harvard Medical School, Boston, USA

Abstract

Background: Hepatic steatosis (HS) is associated with an increased risk of major adverse cardiovascular events (MACE). However, the underlying mechanisms linking HS to MACE remain incompletely understood. This study aimed to investigate the role of the leukopoietic-arterial axis in mediating the relationship between imaging markers of HS and MACE.

☆This article is part of a Special issue entitled: 'CRLM health' published in Metabolism.

*Corresponding author at: 165 Cambridge St, Suite 400, Boston, MA, 02114-2750, USA. SAbohashem@mgh.harvard.edu (S. Abohashem).

Ethics statement and approval

All clinical and imaging data were anonymized prior to analysis. Patients underwent clinical tests and assessments as part of their routine care. The study protocol was reviewed and approved by the local ethics committee of the Mass General Brigham Institutional Review Board (#2010P001955), Boston, USA.

CRediT authorship contribution statement

Shady Abohashem: Writing – review & editing, Writing – original draft, Visualization, Methodology, Investigation, Funding acquisition, Formal analysis, Data curation, Conceptualization. **Wesam Aldosoky:** Writing – review & editing, Visualization, Software. **Taimur Abbasi:** Writing – review & editing, Software, Methodology. **Tawseef Dar:** Writing – review & editing, Software, Data curation. **Robert Rollings:** Writing – review & editing, Data curation. **Brian Tung:** Writing – review & editing, Software, Data curation. **Basma Hammad:** Writing – review & editing, Methodology, Data curation. **Fatima Saeed:** Writing – review & editing, Formal analysis. **Abdelrahman Ali:** Writing – review & editing, Software, Methodology, Data curation. **Richard A.P. Takx:** Writing – review & editing, Software, Investigation. **Brian B. Ghoshhajra:** Writing – review & editing, Software, Investigation. **Ahmed Tawakol:** Writing – review & editing, Supervision, Funding acquisition, Conceptualization. **Michael T. Osborne:** Writing – review & editing, Supervision, Funding acquisition, Conceptualization.

Methods and materials: This longitudinal retrospective cohort study included 445 individuals without active cancer, liver disease or alcohol abuse, or baseline cardiovascular disease who underwent clinical ^{18}F-FDG-PET/CT imaging. Hepatic glucose uptake (HGU), uptake in the bone marrow (BM) and spleen (as a marker of leukopoiesis), and activity in the aorta (as a measure of arterial inflammation, ArtI) were evaluated. Hepatic and splenic attenuations were analyzed to assess hepatic attenuation index (HAI) and determine nonalcoholic fatty liver disease (NAFLD) status. Metabolic Dysfunction Associated Steatotic Liver disease (MASLD) was defined based on NAFLD status and other metabolic criteria. MACE was adjudicated.

Results: In fully adjusted models, HGU associated with heightened BM (standardized β [95 % confidence interval]: 0.353 [0.276, 0.430], $p < 0.001$) and spleen activities (0.548 [0.475, 0.621], $p < 0.001$) as well as ArtI (0.529 [0.453, 0.605], $p < 0.001$). Similar associations were observed for HAI and MASLD or NAFLD status. Notably, these associations remained significant after adjusting for other confounders and among individuals without MASLD/NAFLD. A total of 28 individuals developed MACE over 4 years median follow-up. Furthermore, the leukopoietic-arterial activity mediated the link between imaging markers of HS (i.e., HGU, HAI, MASLD) and MACE, ($p < 0.05$).

Conclusion: Our study suggests an important role for the leukopoietic-arterial axis in HS and MACE. These findings may inform therapeutic avenues for reducing the cardiovascular risk associated with HS.

Structured abstract: This study examines the connection between hepatic steatosis (HS) and major adverse cardiovascular events (MACE) through the leukopoietic-arterial axis. Among 445 patients without history of liver disease or alcohol abuse, imaging markers of hepatic steatosis (i.e., hepatic glucose uptake (HGU)), and metabolic dysfunction associated steatotic liver disease (MASLD), associated with increased activity in bone marrow and spleen, and atherosclerotic plaques. These associations persisted irrespective of MASLD status and after adjusting for relevant confounders. Heightened uptake in leukopoietic tissues and the arteries mediated the relationship between HS markers (i.e., HGU, MASLD) and MACE development. These findings shed light on novel mechanistic pathways and potential targets for interventions to reduce the burden of HS-related CVD.

Keywords

Hepatic steatosis; Non-alcoholic fatty liver disease; Major adverse cardiovascular events; Arterial inflammation; Leukopoietic-arterial axis; Mediation; Metabolic dysfunction associated steatotic liver disease

1. Introduction

Hepatic steatosis (HS), an increasingly common condition manifested by hepatic lipid deposition, represents the earliest stage of disease that can ultimately develop into metabolic dysfunction associated steatotic liver disease (MASLD) as well as a more advanced form of disease that leads to hepatic inflammation (i.e., nonalcoholic steatohepatitis, NASH) [1–5]. HS, and its severe form NASH, are independently associated with a substantial risk of cardiovascular disease (CVD) [1,2]. While a subset of patients with HS may progress to

severe liver disease, CVD remains the primary cause of mortality in individuals with HS [1,2,6]. Nevertheless, the precise mechanisms linking HS to CVD are not fully understood.

Prior research has proposed several mechanisms that underlie the connection between HS and CVD. HS is associated with greater visceral adiposity, atherogenic dyslipidemia, oxidative stress, endothelial dysfunction, and insulin resistance [6–8]. However, the diagnosis of HS confers a greater CVD risk than these factors alone can fully explain [6]. Therefore, uncovering additional pathobiological mechanisms has the potential to provide opportunities to mitigate the burden of CVD associated with HS.

Key physiological functions of the liver, including glucose and lipid metabolism, are disturbed in HS and may contribute to heightened systemic inflammation. This inflammatory milieu arises in part by liver-secreted pro-inflammatory cytokines and molecules [7,9]. The resulting hepatic inflammation can have detrimental effects on the vasculature, leading to vascular damage and disruptions in the coagulation system [8]. Furthermore, prolonged exposure to these inflammatory signals exerts adverse effects on the leukopoietic system, including increased cell proliferation and DNA damage [10]. Notably, recent prospective studies have shown bone marrow (BM) activation in response to the metabolic syndrome [11], but the specific impact of HS on leukopoiesis and arterial inflammation, both of which have been linked to major adverse cardiovascular events (MACE) [11–16], remains unknown.

To bridge this knowledge gap, we leveraged multi-system ^{18}F-fluorodeoxyglucose positron emission tomography/computed tomography (^{18}F-FDG-PET/CT) imaging. This approach utilizes ^{18}F-FDG, a radioactive glucose analogue, to visualize inflammation and metabolic activity in various tissues simultaneously. ^{18}F-FDG-PET/CT allows the assessment of hepatic glucose uptake (HGU), an imaging measure that associates with liver inflammation and has previously been shown to be higher in males than females [3,4,17–20]. In addition, this technique allows quantification of the ^{18}F-FDG signal intensity within the BM and spleen, which is impacted by enhanced leukopoietic function, as well as within the arterial wall, a measure of arterial inflammation (ArtI) [12–15]. Complementing the PET component, CT imaging enables the quantitative evaluation of hepatic and splenic attenuation, thereby facilitating an assessment of HS [21]. Thus, this imaging technique offers a unique opportunity to study the multi-system pathway linking HS to CVD.

Accordingly, in this retrospective study we sought to test the following hypotheses: 1) imaging markers of HS independently associate with elevated leukopoietic tissue activity in the bone marrow and spleen, 2) imaging markers of HS independently associate with heightened ArtI, and 3) the activated leukopoietic-arterial axis mediates the link between imaging markers of HS and MACE. Additionally, in a secondary analysis we will examine whether these associations persist after excluding individuals meeting diagnostic criteria for MASLD. Further, in an exploratory analysis, we will evaluate the sex differences in the association between HGU and MACE.

2. Methods

2.1. Study design and cohort

The study design included a longitudinal retrospective cohort of 445 individuals who underwent full body ^{18}F-FDG-PET/CT imaging for clinical purposes (mainly cancer screening or surveillance) at Massachusetts General Hospital (Boston, MA) between 2005 and 2008 (Fig. 1). The cohort included all consecutive individuals with ^{18}F-FDG-PET/CT imaging that included the liver who did not have a history of clinical CVD, alcohol abuse, liver disease, or evidence of active oncologic or inflammatory diseases at the time of imaging (or during follow-up). Additional inclusion criteria included the availability of at least three clinical visit notes (covering ≥1 year) after the time of index imaging to facilitate adequate clinical follow-up. Detailed inclusion/exclusion criteria were previously published and are included in the Supplemental Methods. The study protocol was approved by the Mass General Brigham Institutional Review Board. Due to the retrospective study design and use of de-identified medical records, the requirement for individual written informed consent was waived.

2.2. Assessment of hepatic steatosis and hepatic glycolytic activity

A trained radiologist who was blinded to all clinical data performed image analysis. Hepatic and splenic attenuations were analyzed using validated methods [21,22]. Hepatic attenuations were measured on non-contrast CT images by manually drawing a standard region of interest (ROI; minimum 2 cm^2) in the axial view at three different levels in the hepatic parenchyma while avoiding hepatic vasculature and biliary structures. The mean Hounsfield unit (HU) value of the three measurements was quantified. Splenic attenuation was measured by manually drawing a standard ROI of a minimum of 2 cm^2 in the axial view at three different levels in the splenic parenchyma, and a mean HU value was derived from the three measurements. Hepatic attenuation index (HAI) was derived from the difference between mean hepatic and splenic attenuations [21,22]. Using previously validated methods, HAI was employed as a diagnostic parameter for non-alcoholic fatty liver disease (NAFLD), characterized by an HAI value less than 1 HU [21,22]. Additionally, MASLD was assessed based on NAFLD status and other metabolic criteria [23,24]. Specifically, the MASLD criteria are based on evidence of hepatic steatosis (imaging or biopsy, and in the absence of excessive alcohol consumption, chronic viral hepatitis, or other competing causes of hepatic steatosis), and meeting any of the cardiometabolic criteria in adults (Supplemental Methods) [23,24]. While individuals diagnosed with NAFLD and no liver disease who do not meet the MASLD criteria are termed ‘cryptogenic steatotic liver disease [SLD] [23,24]. HGU was determined by recording the liver ^{18}F-FDG uptake values for each standard ROI drawn manually as previous described [17,25]. For each individual, the maximum derived standardized uptake values (SUVs) per slice were averaged and then adjusted for mean background venous blood activity from the superior vena cava (SVC) to calculate the target-to-background ratio (TBR). Details about the ^{18}F-FDG-PET/CT imaging protocol are provided in the supplement.

2.3. Measurement of leukopoietic activity and arterial inflammation

Arterial inflammation and BM/splenic (i.e., leukopoietic) activities were measured using previously validated methods by an investigator blinded to clinical data [16]. Briefly, ArtI was assessed by measuring the ^{18}F-FDG signal within the wall of the ascending aorta from 1 cm above the aortic annulus in the axial plane and every 3 mm to the aortic arch. The maximum derived SUVs per slice were averaged and then adjusted for mean background venous blood activity from the SVC to calculate the TBR. Similarly, BM activity is assessed by quantifying the average of the maximum SUVs from ROIs in the vertebral bodies (T1–L5), and splenic activity was assessed by deriving the average of the maximum SUVs from five ROIs in the spleen. BM and splenic activities were corrected for mean SVC activity to yield TBRs.

2.4. Adjudication of clinical outcomes

Clinical outcomes were defined in accordance with those of the Framingham Heart Study and were adjudicated from clinical records by two cardiologists blinded to imaging data [26]. MACE was defined as a composite of non-fatal myocardial infarction, unstable angina, coronary or peripheral revascularization, or cerebrovascular accident within five years of index imaging. Participants were censored upon their first MACE event or last available clinical note. Patients were followed up from index imaging until 2013 to evaluate 5-year MACE risk (primary analysis) and until 2018 for 10-year MACE risk (secondary analysis). Additional details on events adjudication are provided (Supplemental Methods).

2.5. Clinical data and covariables

An electronic medical record review was performed to derive clinical and demographic data. Body mass index (BMI) (kg/m^2) was calculated (using height and weight at the time of PET imaging), and traditional CVD risk factors (i.e., age, sex, hypertension, smoking status, dyslipidemia, and diabetes), statin use, history of cancer or chemotherapy/radiation were gathered. Baseline prediabetes status and antidiabetic medications (i.e. oral hypoglycemic/insulin treatment) were also collected from medical records. On baseline attenuation correction CT images, visceral adipose tissue (VAT) was measured as the volume of adipose tissue with HU from −195 to −45 using the abdominal, inter-costal, and paraspinal musculature as boundaries on a single 3 mm slice at the level of the umbilicus [27]. Subcutaneous adipose tissue (SAT) was measured as a tissue of the same radiographic density within the subcutaneous space. VAT/SAT ratio, a known correlate of metabolic disease, was quantified [28]. Blood lipids including total cholesterol, low density lipoprotein (LDL), high density lipoprotein (HDL), and triglycerides, were collected from medical records at imaging index and were available for 218 subjects.

2.6. Statistical analysis

Continuous variables are provided as mean and standard deviation or when skewed as median and interquartile range (IQR). Normality of continuous variables was assessed using the Shapiro–Wilk test. Independent *t*-tests, Mann-Whitney *U* test, and Chi-square were used, as appropriate, to assess the difference in baseline characteristics between MASLD versus Non-MASLD groups. Imaging markers of HS, leukopoietic and arterial

inflammation parameters were standardized around the mean and presented as z-scores. The associations with BM and splenic activities and ArtI were tested using univariable and multivariable linear regression models yielding a β coefficient with 95 % confidence intervals (CIs). Multivariable models were specified a priori. The primary model included traditional CVD risk factors (i.e., age, sex, hypertension, smoking, dyslipidemia, and diabetes), BMI, and statin use. Other models included age, sex, VAT/SAT ratio, blood lipids, history of malignancy and chemotherapy or radiation. MASLD status was used for primary analyses, and a sensitivity analysis for NAFLD was conducted. Cox regression and Kaplan-Meier curve survival analysis were used to test the relationship between HGU and MACE (at 5 and 10 years) and provide hazard ratios (HRs). Assumptions for Cox regression were verified using the Schoenfeld residuals test. Because males have higher HGU than females [20], an exploratory analysis was conducted to evaluate the sex effect modification on the relationship between HGU and MACE. Mediation analyses were used to test the hypothesized mechanistic path: imaging markers of HS→^{18}F-FDG uptake in leukopoietic tissues→ArtI→MACE in age and sex adjusted models [29]. Additional details about mediation analyses are described in the Supplemental Methods. For missing data, complete-case analyses were performed. Statistical analyses were performed using SPSS (version 29, IBM Corporation, Armonk, NY), all tests were two-tailed, and a p-value <0.05 indicated statistical significance.

2.7. Validation cohort

To further assess our findings, we performed a validation analysis within a subset of participants from the primary cohort who underwent a second clinical ^{18}F-FDG-PET/CT scan within one year of the index imaging. Similarly, these repeat scans were performed for cancer screening or surveillance purposes, with no evidence of active malignancy at baseline or during the follow-up scan. A total of 26 subjects met these criteria and were included in this supplemental analysis.

For these individuals, HGU, BM and splenic activities, and ArtI were re-measured at the follow-up scan using the same protocols applied to the index scan. Associations between HGU and leukopoietic/arterial activity at follow-up were tested using both univariable and multivariable linear regression models. The primary multivariable model adjusted for traditional cardiovascular disease risk factors (age, sex, smoking, diabetes, hyperlipidemia, hypertension), BMI, statin use, and baseline HGU (to account for regression to the mean and individual-level differences at the index imaging). All continuous variables were standardized around the mean and presented as z-scores.

2.7.1. Patient and public involvement: Patients and/or the public were not involved in the design, conduct, reporting, or dissemination plans of this research.

3. Results

3.1. Baseline characteristics

A total of 445 individuals were included with a median age (IQR) of 55 (44–66) years, and 43.6 % were male. Among the participants, 70 individuals met CT-based criteria for

NAFLD (67 met criteria for MASLD and 3 for cryptogenic SLD), MASLD was associated with a higher prevalence of several CVD risk factors compared to those without MASLD (Table 1). Additionally, individuals with MASLD exhibited higher BMI, VAT, SAT, and HGU compared to those without MASLD.

3.2. Associations between imaging markers of HS and leukopoietic activity

In a primary model adjusted for CVD risk factors, BMI, and statin use, HGU significantly associated with heightened BM (standardized β [95 % CI]: 0.353 [0.276, 0.430], $p < 0.001$) and splenic activities (0.548 [0.475, 0.621], $p < 0.001$; Fig. 2). Similarly, both MASLD status and absolute HAI were significantly associated with increased BM (0.349 [0.076, 0.623], $p = 0.012$ and −0.186 [−0.271, −0.101], $p < 0.001$); respectively) and splenic activities (0.491 [0.210, 0.772], $p < 0.001$ and −0.204 [−0.294, −0.114], $p < 0.001$); respectively) in multivariable models including fully adjusted model.

These associations remained significant for NAFLD status, after adjusting for additional relevant confounders (Table 2), and after excluding individuals with MASLD or NAFLD (Supplemental Table 1, Supplemental Fig. 2).

3.3. Associations between imaging markers of HS and arterial inflammation

In a primary model adjusted for CVD risk factors, BMI, and statin use, heightened ArtI was significantly associated with HGU, HAI, and MASLD (standardized β [95 % CI]: 0.529 [0.453, 0.605], $p < 0.001$; −0.116 [−0.207, −0.025], $p = 0.012$; and 0.291 [0.026, 0.556], $p = 0.031$, respectively; Fig. 3, Table 2). Importantly, heightened ArtI remained significantly associated with HGU, HAI, and MASLD (standardized β [95 % CI]: 0.563 [0.441, 0.685], $p < 0.001$; −0.180 [−0.349, −0.011], $p = 0.037$; and 0.507 [0.062, 0.953], $p = 0.026$, respectively) after adjustment for age, sex, VAT/SAT ratio, and blood lipids (i.e., total cholesterol, LDL, HDL, and triglycerides). Similar associations were observed with NAFLD and after adjusting for additional covariables including fully adjusted model (Table 2). Importantly, these associations persisted after excluding subjects with MASLD or NAFLD (Supplementary Table 1, Supplemental Fig. 2).

3.4. Validation cohort

Among the 26 individuals with repeat ^{18}F-FDG-PET/CT imaging within one year of baseline, the median (IQR) age was 57 (46–69) years, and 34.6 % were male. In this subset, HGU at follow-up remained significantly associated with leukopoietic and arterial tissue activities. In univariable models, higher HGU was associated with greater ArtI (standardized β = 0.529, 95 % CI: 0.179–0.879, $p = 0.005$), BM activity (β = 0.502, 95 % CI: 0.059–0.945, $p = 0.029$), and splenic activity (β = 0.666, 95 % CI: 0.288–1.045, $p = 0.002$). Importantly, these associations persisted in the multivariable model adjusted for cardiovascular risk factors, BMI, statin use, and baseline HGU (Supplemental Table 2).

3.5. Association between HGU and incident MACE

A total of 28 individuals experienced MACE during a median follow-up of 4.0 years, while 64 individuals experienced MACE over median 10 years follow up. After adjusting for CVD risk factors, BMI, and statin use, HGU was associated with higher 5-year MACE risk

(standardized HR (95 % CI): 1.516 [1.101, 2.086], $p = 0.011$) as well as 10-year MACE risk (1.370 [1.065, 1.761], $p = 0.014$; Fig. 4A–B). Similar associations were observed after adjusting for additional confounders, including fully adjusted model (Fig. 4A). Importantly, the association between HGU and MACE remained significant after excluding individuals with MASLD or NALFD (5-year MACE: 1.634 [1.115, 2.398], $p = 0.012$; 10-year MACE: 1.496 [1.106, 2.025], $p = 0.009$). Notably, the association between HGU and MACE was also stronger (~4 times) among males (standardized HR (95 % CI): 2.135 [1.254, 3.365], $p = 0.005$) compared to females (1.233 [0.762, 1.994], $p = 0.393$); p-interaction = 0.001) in a model adjusted for CVD risk factors, BMI, and statin use. Consistent with previous evidence [11–16], leukopoietic activity in the BM and spleen associated with ArtI, and both independently associated with incident MACE (Supplemental Table 3).

3.6. The leukopoietic-arterial axis mediates the link between imaging markers of HS and MACE

Given the observed associations between HGU and leukopoietic-arterial activity as well as their relationships with MACE (Table 2, Figs. 2 & 3, Supplemental Table 3), we conducted a mediation analysis to investigate the mediating role of activities of leukopoietic organs and the arterial wall in linking HGU to MACE. This mediation analysis, adjusted for age and sex, revealed a significant mediating effect of the hypothesized pathway [HGU→^{18}F-FDG uptake in the BM →^{18}F-FDG uptake in the spleen→ ArtI→MACE] ($p < 0.05$) (Fig. 5). Additionally, similar mediation models demonstrated a mediating role of the [BM →Spleen →ArtI] axis in connecting MASLD/NAFLD and HAI to MACE (Supplemental Fig. 3). The mediating effect of the [BM →Spleen →ArtI] axis in linking HGU and HAI to MACE persisted even after excluding individuals with MASLD/NAFLD (Supplemental Fig. 4).

4. Discussion

The present study leveraged multi-system ^{18}F-FDG-PET/CT imaging to investigate the link between hepatic steatosis and major adverse cardiovascular events. The findings shed light on novel underlying mechanisms by identifying associations between imaging markers of HS, including HGU and HAI, and key factors associated with CVD, such as heightened ^{18}F-FDG uptake, a marker of leukopoietic activity, in the bone marrow and spleen as well as increased ^{18}F-FDG uptake in the arterial wall, a marker of atherosclerotic inflammation. These associations remained after accounting for important confounders and persisted even among individuals who did not meet radiographic criteria for MASLD/NAFLD. Moreover, our results suggest a mediating role of the leukopoietic-arterial axis in linking HS to MACE, and irrespective of MASLD/NAFLD status. These findings highlight important pathobiological mechanisms underlying HS-related CVD.

4.1. Imaging phenotypes of HS as a marker of CVD risk

NAFLD, a distinct form of HS, is frequently evaluated using HAI [21,22]. Both MASLD, NAFLD (and its continuous counterpart, HAI), are strongly associated with heightened cardiometabolic and CVD risks [1,2,5,30,31]. The magnitude of that risk parallels the underlying disease severity, such that patients with NASH, a progressive form of NAFLD associated with histological inflammation and cell injury, have greater risk of atherosclerotic

CVD [30,32]. Therefore, ^{18}F-FDG-PET imaging has emerged as a technique that provides an assessment that associates with hepatic inflammation through the measurement of HGU [17,33–39]. While other factors can impact the uptake of ^{18}F-FDG in the liver, activated inflammatory cells have an increased affinity for ^{18}F-FDG and contribute to increased radiotracer uptake in the liver with the magnitude of uptake serving as an indicator of inflammation severity [3,17,36,38]. In addition, prior research and the current findings (Supplemental Fig. 5) have identified increased hepatic ^{18}F-FDG uptake in association with both MASLD and NAFLD [3,39,40]. Notably, this heightened uptake correlates with other hepatic inflammation and injury markers, including triglyceride and gamma-glutamyl transferase levels, independent of the presence of NAFLD [3,38–41]. Our findings that HGU associates with imaging measures related to CVD risk (i.e., leukopoietic-arterial activity) even in the absence of MASLD/NAFLD diagnosis, reinforce the notion that HGU holds potential as a clinically meaningful marker of hepatic inflammation.

4.2. Independent association between HGU and MACE

While the association between MASLD/NAFLD and MACE is established [1,2], there is scant evidence connecting HGU to MACE. A previous study suggested a connection between HGU and MACE only in the presence of both NAFLD and elevated HGU, failing to establish an independent association [32,34,35]. Limitations in sample size, suboptimal imaging techniques, and limited event rates to allow adjustment for key confounders have precluded conclusive results [32,34,35]. In contrast, our current study is the first to identify a direct link between HGU and increased MACE risk, even after controlling for known CVD risk factors, measures of adiposity, malignancy, and related treatment. Importantly, this association persisted even among individuals without MASLD/NAFLD or any clinical liver disease, underscoring the prognostic utility of HGU in predicting CVD irrespective of MASLD/NAFLD status.

Prior studies have indicated higher HGU levels in males than females [20]. This finding prompted us to study the sex influence on the association between HGU and MACE. Intriguingly, we found notable sex differences wherein males experienced almost four-fold higher risk of MACE associated with HGU compared to females. This finding underscores the need to further explore sex-specific factors influencing the liver-heart axis in future research.

4.3. Mechanistic insights

HS has been linked to vascular dysfunction including carotid intima thickness and subclinical atherosclerosis [42], but limited data exist on its connection to arterial ^{18}F-FDG uptake as a marker of ArtI. A small study of 151 individuals explored the relationship between NAFLD and ArtI; however, this association was attenuated after adjusting for body fat and low density lipoprotein cholesterol, likely due to the study's limited sample size [31]. In the larger current investigation, we link it for first time to the newly defined MASLD and establish that this association is indeed independent of body fat and cholesterol levels. Furthermore, our findings suggest a multi-tissue mechanism linking HS to CVD, through enhanced uptake of ^{18}F-FDG in leukopoietic tissues and the arteries that has similarly been

implicated in several other pathologies that associate with heightened CVD risk (Graphical Abstract) [43–46].

Hepatic lipid deposition leads to subacute hepatic inflammation, accompanied by accumulation of inflammatory leukocytes and increased hepatic and extrahepatic cytokine/chemokines production (in particular TNF-α, IL-6, IL-1, CRP) [47,48]. Activation of inflammatory pathways, such as the NF-kB pathway and the NLRP3 inflammasome, triggers the release of inflammatory mediators, promoting the transcription of pro-inflammatory genes and driving systemic, low-grade inflammation [49,50]. The persistence of these inflammatory signals adversely affects leukopoiesis, leading to increased cell proliferation and DNA damage [10,51–53]. Our subgroup analyses further indicate that these inflammatory and leukopoietic effects extend even to individuals without MASLD/NAFLD, suggesting that subclinical hepatic metabolic alterations may activate systemic inflammatory pathways, supporting a broader hepatic–metabolic–inflammatory axis. In addition, NAFLD-related metabolic dysregulation may impair the bone marrow microenvironment and bone remodeling, potentially linking hepatic steatosis to reduced bone mineralization, as suggested in prior work [54]. Animal studies have further highlighted the association between obesity and abnormal cholesterol levels to heightened proliferation and activity of leukopoietic cells in These BM [51,52,55,56]. These conditions are linked to increased neutrophilia and monocytosis, exacerbating inflammation and promoting the development of atherosclerosis [51,52,55,56]. Supporting this, recent research has demonstrated heightened BM activity in association with other components of the metabolic syndrome without specifically including NAFLD in their analysis or definition of the metabolic syndrome. That study further demonstrated a significant association between BM activity and higher arterial metabolic activity, a marker of inflammatory atherosclerosis [11].

Although our primary analysis was cross-sectional in nature, we sought to validate these findings in a subset of individuals from our cohort who underwent repeat ^{18}F-FDG-PET/CT imaging within one year. Among 26 participants without evidence of active malignancy, HGU at the follow-up scan remained consistently associated with ArtI, BM, and splenic activity, even after adjustment for traditional risk factors, and baseline HGU. These reproducible associations across two imaging time points, albeit in a small subset, support the robustness of our main observations and suggest that HGU is not merely a transient finding but rather reflects a measure related to hepatic steatosis that consistently associates with leukopoietic activation and arterial inflammation. Prospective studies with serial imaging at standardized intervals, and detailed inflammatory biomarker assessments will be critical to further substantiate and define these multi-tissue pathways.

4.4. Study limitations

Several limitations of our work should be acknowledged. First, the retrospective study design may have introduced potential biases; however, the use of comprehensive medical records and validated imaging techniques help to overcome these limitations. Because ^{18}F-FDG-PET/CT imaging was originally performed for oncologic screening or surveillance, selection bias is possible despite our exclusion of individuals with active cancer or

inflammatory conditions. Accordingly, validation in prospective, population-based cohorts remains important to confirm generalizability. While efforts were made to adjust for confounding factors, residual confounding cannot be completely ruled out. Given the liver's critical role in glucose metabolism and storage, hepatic ^{18}F-FDG uptake may not be solely due to inflammation. Nevertheless, the measure remained independently associated with arterial inflammation and an increased risk of CVD, suggesting that it remains a useful marker of CVD risk. In addition, although we lacked an external validation cohort, a small subset of participants with repeat imaging showed consistent findings, providing internal support for our results. Furthermore, the study did not fully elucidate the specific molecular pathways involved, highlighting the need for further investigation using cellular, molecular, and genetic analyses. We also lacked uniform data on liver fibrosis (e.g., FIB-4, NFS, elastography), limiting our ability to assess its independent contribution to cardiovascular risk; future studies should address this. Lastly, the absence of liver biopsy may have introduced misclassification or underestimation of hepatic steatosis prevalence and severity, but the imaging measures utilized in this study have been validated and are widely used in clinical practice. Future research should incorporate prospective studies of large and diverse populations to enhance the robustness and generalizability of the findings.

4.5. Future directions and clinical implications

Future studies should be designed to further clarify the mechanisms linking HS to MACE and evaluate the impact of therapies on this relationship. Prospective studies would be needed to confirm these findings. A key opportunity involves the identification of novel therapeutic targets that act on the intermediaries linking HS to MACE. Potential approaches targeting this pathway include pharmaceutical agents that directly affect arterial inflammation and leukopoiesis, such as statins or anti-inflammatory drugs [57,58]. A recent prospective study showed a reduction in BM and splenic ^{18}F-FDG uptake in response to atorvastatin among people with type 2 diabetes [58]. Further, animal studies have shown that exercise and healthy sleep duration attenuate BM leukopoietic activity and atherosclerosis, implying that lifestyle modifications may attenuate CVD risk associated with HS by influencing the leukopoietic-arterial axis [43,44]. Understanding the specific molecular mechanisms underlying these pathways is crucial for designing precise and effective therapies. Additionally, the impact of targeted interventions to reduce HS on these mechanisms should be explored.

5. Conclusion

Imaging markers of hepatic steatosis, namely HGU and HAI, are associated with factors implicated in cardiovascular pathology including heightened leukopoietic activity in the bone marrow and spleen and increased arterial inflammation. These associations remained robust even among individuals who did not meet metabolic and imaging criteria for MASLD/NAFLD, reinforcing their clinical relevance beyond traditional diagnostic criteria. Our findings suggest an important role for the leukopoietic-arterial axis in linking HS to MACE and provide a foundation for future investigations and potential therapeutic interventions.

Supplementary Material

Refer to Web version on PubMed Central for supplementary material.

Funding

SA is supported in part by faculty development award (Shore Program 2023) by Harvard Medical School (HMS) - Radiology department of Mass General Hospital, and American Heart Association (AHA) (#24SCEFIA1256969). MTO is supported in part by National Institutes of Health (NIH) K23HL151909, AHA 23SCISA1143491, and the generosity of the Hassenfeld family. AT is supported in part by NIH R01AR077187, R33HL141047, R01HL152957, R01HL149516, and R01HL164337.

Declaration of competing interest

Dr. Abohashem and Dr. Osborne analyzed and controlled the data. Dr. Osborne receives consulting fees from WCG Clinical and serves as an expert witness for Quiet Communities for unrelated work. All other authors have reported that they have no relationships relevant to the contents of this paper to disclose.

Appendix A.: Supplementary data

Supplementary data to this article can be found online at https://doi.org/10.1016/j.metabol.2025.156427.

Data availability

Deidentified data will be available on reasonable request.

Abbreviations:

HGU	hepatic glucose uptake
MACE	major adverse cardiovascular events
NAFLD	non-alcoholic fatty liver disease
^{18}F-FDG-PET/CT	^{18}F-fluorodeoxyglucose positron emission tomography/computed tomography
ArtI	arterial inflammation
BM	bone marrow
HAI	hepatic attenuation index
HS	hepatic steatosis
CVD	cardiovascular disease
MASLD	metabolic dysfunction associated steatotic liver disease

References

[1]. Targher G, Byrne CD, Tilg H. NAFLD and increased risk of cardiovascular disease: clinical associations, pathophysiological mechanisms and pharmacological implications. Gut Sep 2020;69(9):1691–705. 10.1136/gutjnl-2020-320622. [PubMed: 32321858]

[2]. Adams LA, Anstee QM, Tilg H, Targher G. Non-alcoholic fatty liver disease and its relationship with cardiovascular disease and other extrahepatic diseases. Gut Jun 2017;66(6):1138–53. 10.1136/gutjnl-2017-313884. [PubMed: 28314735]

[3]. Keramida G, Potts J, Bush J, Verma S, Dizdarevic S, Peters AM. Accumulation of (18)F-FDG in the liver in hepatic steatosis. AJR Am J Roentgenol Sep 2014;203(3): 643–8. 10.2214/ajr.13.12147. [PubMed: 25148170]

[4]. Zhaoting M, Gang F, Min Z, et al. Accumulation of ^{18}F-FDG in the liver in metabolic associated fatty liver disease detected on PET/MR. J Nucl Med 2021;62(supplement 1):1023.

[5]. Duell PB, Welty FK, Miller M, et al. Nonalcoholic fatty liver disease and cardiovascular risk: a scientific statement from the American Heart Association. Arterioscler Thromb Vasc Biol 2022;42(6):e168–85. 10.1161/ATV.0000000000000153. [PubMed: 35418240]

[6]. Allen AM, Therneau TM, Larson JJ, Coward A, Somers VK, Kamath PS. Nonalcoholic fatty liver disease incidence and impact on metabolic burden and death: a 20 year-community study. Hepatology May 2018;67(5):1726–36. 10.1002/hep.29546. [PubMed: 28941364]

[7]. Al Rifai M, Silverman MG, Nasir K, et al. The association of nonalcoholic fatty liver disease, obesity, and metabolic syndrome, with systemic inflammation and subclinical atherosclerosis: the Multi-Ethnic Study of Atherosclerosis (MESA). Atherosclerosis Apr 2015;239(2):629–33. 10.1016/j.atherosclerosis.2015.02.011. [PubMed: 25683387]

[8]. Kasper P, Martin A, Lang S, et al. NAFLD and cardiovascular diseases: a clinical review. Clin Res Cardiol Jul 2021;110(7):921–37. 10.1007/s00392-020-01709-7. [PubMed: 32696080]

[9]. Libby P, Everett BM. Novel antiatherosclerotic therapies. Arterioscler Thromb Vasc Biol Apr 2019;39(4):538–45. 10.1161/atvbaha.118.310958. [PubMed: 30816799]

[10]. Leimkühler NB, Schneider RK. Inflammatory bone marrow microenvironment. Hematology Am Soc Hematol Educ Program 2019;2019(1):294–302. 10.1182/hematology.2019000045. [PubMed: 31808897]

[11]. Devesa A, Lobo-González M, Martínez-Milla J, et al. Bone marrow activation in response to metabolic syndrome and early atherosclerosis. Eur Heart J 2022;43(19):1809–28. 10.1093/eurheartj/ehac102. May 14. [PubMed: 35567559]

[12]. Rudd JHF. Imaging atherosclerotic plaque inflammation with [18F]-fluorodeoxyglucose positron emission tomography. Circulation 2002;105(23):2708–11. 10.1161/01.cir.0000020548.60110.76. [PubMed: 12057982]

[13]. Rudd JH, Myers KS, Bansilal S, et al. Atherosclerosis inflammation imaging with 18F-FDG PET: carotid, iliac, and femoral uptake reproducibility, quantification methods, and recommendations. J Nucl Med Jun 2008;49(6):871–8. 10.2967/jnumed.107.050294.

[14]. Tawakol A, Migrino RQ, Bashian GG, et al. In vivo 18F-fluorodeoxyglucose positron emission tomography imaging provides a noninvasive measure of carotid plaque inflammation in patients. J Am Coll Cardiol 2006;48(9):1818–24. 10.1016/j.jacc.2006.05.076. Nov 7. [PubMed: 17084256]

[15]. Tawakol A, Ishai A, Takx RA, et al. Relation between resting amygdalar activity and cardiovascular events: a longitudinal and cohort study. Lancet 2017;389(10071):834–45. 10.1016/s0140-6736(16)31714-7. Feb 25. [PubMed: 28088338]

[16]. Abohashem S, Osborne MT, Dar T, et al. A leucopoietic-arterial axis underlying the link between ambient air pollution and cardiovascular disease in humans. Eur Heart J 2021;42(7):761–72. 10.1093/eurheartj/ehaa982. Feb 14. [PubMed: 33428721]

[17]. Iozzo P, Jarvisalo MJ, Kiss J, et al. Quantification of liver glucose metabolism by positron emission tomography: validation study in pigs. Gastroenterology Feb 2007;132(2):531–42. 10.1053/j.gastro.2006.12.040. [PubMed: 17258736]

[18]. Gullberg GT, Shrestha UM, Seo Y. PET imaging of glucose and fatty acid metabolism for NAFLD patients. J Nucl Cardiol 2020;27(5):1689–97. 10.1007/s12350-018-01532-8. 2020/10/01. [PubMed: 30547298]

[19]. Sarikaya I, Schierz JH, Sarikaya A. Liver: glucose metabolism and 18F-fluorodeoxyglucose PET findings in normal parenchyma and diseases. Am J Nucl Med Mol Imaging 2021;11(4):233–49. [PubMed: 34513277]

[20]. Keramida G, Peters AM. Fasting hepatic glucose uptake is higher in men than women. Physiol Rep Jun 2017;5(11). 10.14814/phy2.13174.

[21]. Park YS, Park SH, Lee SS, et al. Biopsy-proven nonsteatotic liver in adults: estimation of reference range for difference in attenuation between the liver and the spleen at nonenhanced CT. Radiology Mar 2011;258(3):760–6. 10.1148/radiol.10101233. [PubMed: 21212369]

[22]. Meyersohn NM, Mayrhofer T, Corey KE, et al. Association of hepatic steatosis with major adverse cardiovascular events, independent of coronary artery disease. Clin Gastroenterol Hepatol Jul 2021;19(7):1480–1488.e14. 10.1016/j.cgh.2020.07.030. [PubMed: 32707340]

[23]. Rinella ME, Lazarus JV, Ratziu V, et al. A multi-society Delphi consensus statement on new fatty liver disease nomenclature. Hepatology 9900:10.1097/HEP.0000000000000520. doi:https://doi.org/10.1097/hep.0000000000000520.

[24]. Eslam M, Newsome PN, Sarin SK, et al. A new definition for metabolic dysfunction-associated fatty liver disease: an international expert consensus statement. J Hepatol Jul 2020;73(1):202–9. 10.1016/j.jhep.2020.03.039. [PubMed: 32278004]

[25]. Viner M, Mercier G, Hao F, Malladi A, Subramaniam RM. Liver SULmean at FDG PET/CT: interreader agreement and impact of placement of volume of interest. Radiology May 2013;267(2):596–601. 10.1148/radiol.12121385. [PubMed: 23297330]

[26]. D'Agostino RB Sr, Vasan RS, Pencina MJ, et al. General cardiovascular risk profile for use in primary care: the Framingham Heart Study. Circulation 2008;117(6):743–53. 10.1161/circulationaha.107.699579. Feb 12. [PubMed: 18212285]

[27]. Maurovich-Horvat P, Massaro J, Fox CS, Moselewski F, O'Donnell CJ, Hoffmann U. Comparison of anthropometric, area- and volume-based assessment of abdominal subcutaneous and visceral adipose tissue volumes using multi-detector computed tomography. Int J Obes (Lond) Mar 2007;31(3):500–6. 10.1038/sj.ijo.0803454. [PubMed: 16953256]

[28]. Kaess BM, Pedley A, Massaro JM, Murabito J, Hoffmann U, Fox CS. The ratio of visceral to subcutaneous fat, a metric of body fat distribution, is a unique correlate of cardiometabolic risk. Diabetologia Oct 2012;55(10):2622–30. 10.1007/s00125-012-2639-5. [PubMed: 22898763]

[29]. Hayes AF. Introduction to mediation, moderation, and conditional process analysis: A regression-based approach. Guilford publications; 2017.

[30]. Stahl EP, Dhindsa DS, Lee SK, Sandesara PB, Chalasani NP, Sperling LS. Nonalcoholic fatty liver disease and the heart. J Am Coll Cardiol 2019;73(8):948–63. 10.1016/j.jacc.2018.11.050. [PubMed: 30819364]

[31]. Lee HJ, Lee CH, Kim S, et al. Association between vascular inflammation and nonalcoholic fatty liver disease: analysis by (18)F-fluorodeoxyglucose positron emission tomography. Metabolism Feb 2017;67:72–9. 10.1016/j.metabol.2016.11.004. [PubMed: 28081780]

[32]. Moon SH, Hong SP, Cho YS, et al. Hepatic FDG uptake is associated with future cardiovascular events in asymptomatic individuals with non-alcoholic fatty liver disease. J Nucl Cardiol Jun 2017;24(3):892–9. 10.1007/s12350-015-0297-y. [PubMed: 26510948]

[33]. Verloh N, Einspieler I, Utpatel K, et al. In vivo confirmation of altered hepatic glucose metabolism in patients with liver fibrosis/cirrhosis by (18)F-FDG PET/CT. EJNMMI Res 2018;8(1):98. 10.1186/s13550-018-0452-y. Nov 9. [PubMed: 30414009]

[34]. Dimitriu-Leen AC, Scholte A. Hepatic FDG uptake in patients with NAFLD: an important prognostic factor for cardio-cerebrovascular events? J Nucl Cardiol Jun 2017;24(3):900–2. 10.1007/s12350-015-0380-4. [PubMed: 26728014]

[35]. Sarkar S, Corwin MT, Olson KA, et al. Pilot study to diagnose nonalcoholic steatohepatitis with dynamic 18F-FDG PET. Am J Roentgenol 2019;212(3):529–37. 10.2214/ajr.18.20012. [PubMed: 30673340]

[36]. Bural GG, Torigian DA, Burke A, et al. Quantitative assessment of the hepatic metabolic volume product in patients with diffuse hepatic steatosis and normal controls through use of FDG-PET and MR imaging: a novel concept. Mol Imaging Biol Jun 2010;12(3):233–9. 10.1007/s11307-009-0258-4. [PubMed: 19806406]

[37]. Rudd JH, Warburton EA, Fryer TD, et al. Imaging atherosclerotic plaque inflammation with [18F]-fluorodeoxyglucose positron emission tomography. Circulation 2002;105(23):2708–11. 10.1161/01.cir.0000020548.60110.76. Jun 11. [PubMed: 12057982]

[38]. Nakahara T, Takagi Y, Takemasa K, et al. Dose-related fluorodeoxyglucose uptake in acute radiation-induced hepatitis. Eur J Gastroenterol Hepatol Oct 2008;20(10):1040–4. 10.1097/MEG.0b013e3282f5f5d5. [PubMed: 18787476]

[39]. Meng Z, Feng G, Zhu M, et al. Accumulation of 18F-FDG in the liver in metabolic associated fatty liver disease detected on PET/MR. J Nucl Med 2021;62 (supplement 1):1023.

[40]. Keramida G, Potts J, Bush J, Dizdarevic S, Peters AM. Hepatic steatosis is associated with increased hepatic FDG uptake. Eur J Radiol May 2014;83(5):751–5. 10.1016/j.ejrad.2014.01.027. [PubMed: 24581596]

[41]. Hong SP, Noh TS, Moon SH, et al. Hepatic glucose uptake is increased in association with elevated serum γ-glutamyl transpeptidase and triglyceride. Dig Dis Sci Mar 2014;59(3):607–13. 10.1007/s10620-013-2957-6. [PubMed: 24326630]

[42]. Fargion S, Porzio M, Fracanzani AL. Nonalcoholic fatty liver disease and vascular disease: state-of-the-art. World J Gastroenterol 2014;20(37):13306–24. 10.3748/wjg.v20.i37.13306. Oct 7. [PubMed: 25309067]

[43]. McAlpine CS, Kiss MG, Rattik S, et al. Sleep modulates haematopoiesis and protects against atherosclerosis. Nature Feb 2019;566(7744):383–7. 10.1038/s41586-019-0948-2. [PubMed: 30760925]

[44]. Frodermann V, Rohde D, Courties G, et al. Exercise reduces inflammatory cell production and cardiovascular inflammation via instruction of hematopoietic progenitor cells. Nat Med Nov 2019;25(11):1761–71. 10.1038/s41591-019-0633-x. [PubMed: 31700184]

[45]. Tawakol A, Osborne MT, Wang Y, et al. Stress-associated neurobiological pathway linking socioeconomic disparities to cardiovascular disease. J Am Coll Cardiol 2019;73(25):3243–55. 10.1016/j.jacc.2019.04.042. [PubMed: 31248544]

[46]. Tawakol A, Ishai A, Takx RAP, et al. Relation between resting amygdalar activity and cardiovascular events: a longitudinal and cohort study. The Lancet 2017;389(10071):834–45. 10.1016/s0140-6736(16)31714-7.

[47]. Tilg H, Moschen AR. Evolution of inflammation in nonalcoholic fatty liver disease: the multiple parallel hits hypothesis. Hepatology 2010;52(5):1836–46. 10.1002/hep.24001. [PubMed: 21038418]

[48]. Krenkel O, Tacke F. Liver macrophages in tissue homeostasis and disease. Nat Rev Immunol 2017;17(5):306–21. 10.1038/nri.2017.11. 2017/05/01. [PubMed: 28317925]

[49]. Romics L Jr, Kodys K, Dolganiuc A, et al. Diverse regulation of NF-kappaB and peroxisome proliferator-activated receptors in murine nonalcoholic fatty liver. Hepatology Aug 2004;40(2):376–85. 10.1002/hep.20304. [PubMed: 15368442]

[50]. Targher G, Day CP, Bonora E. Risk of cardiovascular disease in patients with nonalcoholic fatty liver disease. N Engl J Med 2010;363(14):1341–50. 10.1056/NEJMra0912063. Sep 30. [PubMed: 20879883]

[51]. Tolani S, Pagler TA, Murphy AJ, et al. Hypercholesterolemia and reduced HDL-C promote hematopoietic stem cell proliferation and monocytosis: studies in mice and FH children. Atherosclerosis Jul 2013;229(1):79–85. 10.1016/j.atherosclerosis.2013.03.031. [PubMed: 23684512]

[52]. Nagareddy PR, Kraakman M, Masters SL, et al. Adipose tissue macrophages promote myelopoiesis and monocytosis in obesity. Cell Metab 2014;19(5):821–35. 10.1016/j.cmet.2014.03.029. May 6. [PubMed: 24807222]

[53]. Al-Sharea A, Lee MKS, Whillas A, et al. Chronic sympathetic driven hypertension promotes atherosclerosis by enhancing hematopoiesis. Haematologica Mar 2019;104(3):456–67. 10.3324/haematol.2018.192898. [PubMed: 30361420]

[54]. Barchetta I, Lubrano C, Cimini FA, et al. Liver fibrosis is associated with impaired bone mineralization and microstructure in obese individuals with non-alcoholic fatty liver disease. Hepatol Int Apr 2023;17(2):357–66. 10.1007/s12072-022-10461-1.

[55]. Yvan-Charvet L, Pagler T, Gautier EL, et al. ATP-binding cassette transporters and HDL suppress hematopoietic stem cell proliferation. Science 2010;328(5986):1689–93. 10.1126/science.1189731. Jun 25. [PubMed: 20488992]

[56]. Singer K, DelProposto J, Morris DL, et al. Diet-induced obesity promotes myelopoiesis in hematopoietic stem cells. Mol Metab Sep 2014;3(6):664–75. 10.1016/j.molmet.2014.06.005. [PubMed: 25161889]

[57]. Tawakol A, Fayad ZA, Mogg R, et al. Intensification of statin therapy results in a rapid reduction in atherosclerotic inflammationresults of a multicenter fluorodeoxyglucose-positron emission tomography/computed tomography feasibility study. J Am Coll Cardiol 2013;62(10):909–17. 10.1016/j.jacc.2013.04.066. [PubMed: 23727083]

[58]. Oostveen RF, Kaiser Y, Ståhle MR, et al. Atorvastatin lowers 68Ga-DOTATATE uptake in coronary arteries, bone marrow and spleen in individuals with type 2 diabetes. Diabetologia 2023. 10.1007/s00125-023-05990-9. 2023/08/15.

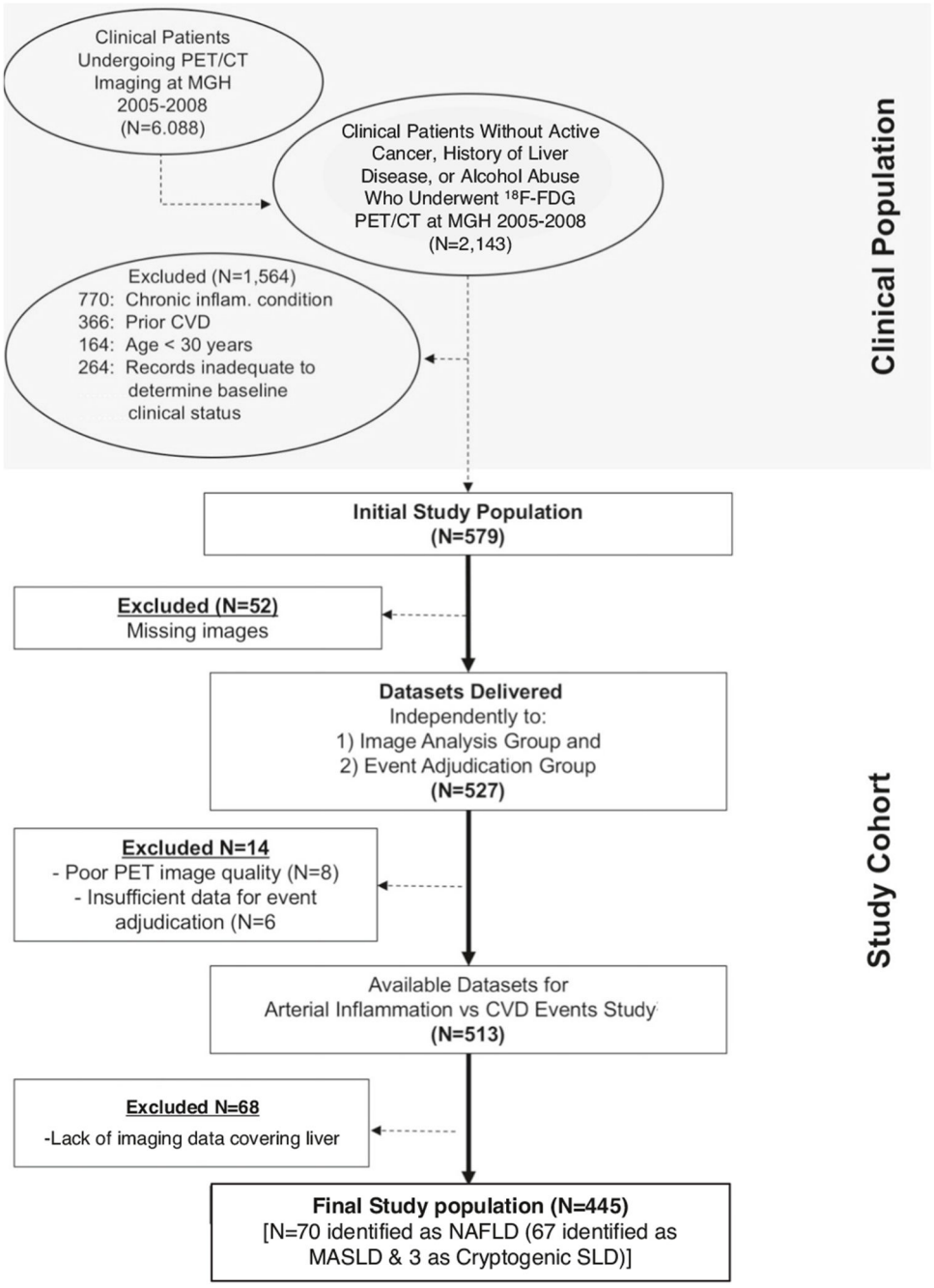

Fig. 1.

Subject selection. Abbreviations: CT-computed tomography, CVD-cardiovascular disease, ^{18}F-FDG-fluorodeoxyglucose, MACE-major adverse cardiovascular event, MGH-Massachusetts General Hospital, PET-positron emission tomography, NAFLD-nonalcoholic fatty liver disease, MASLD-metabolic dysfunction associated steatotic liver disease.

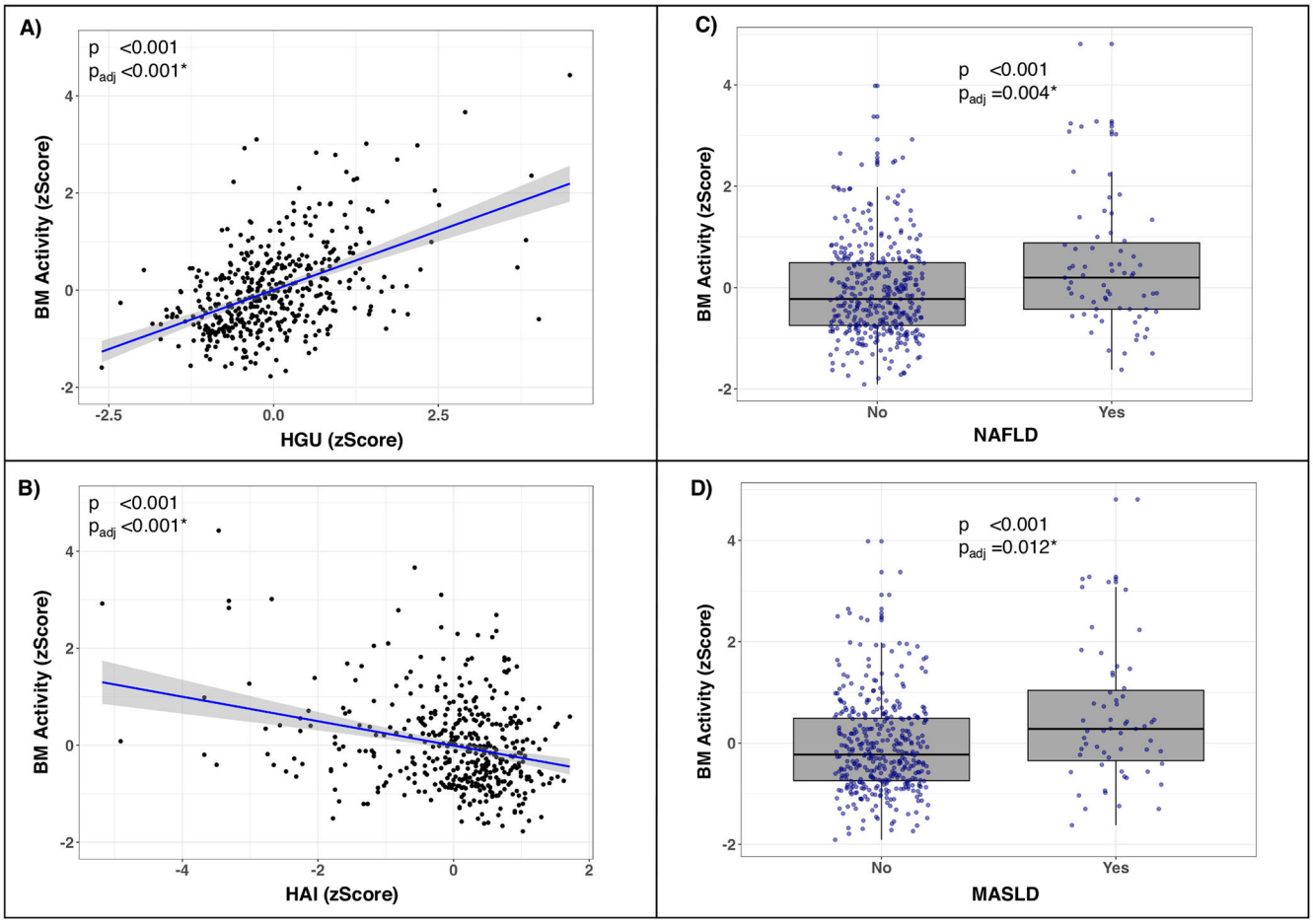

Fig. 2.

Association between imaging markers of hepatic steatosis and BM activity among the entire cohort. * Adjusted for primary model (CVD risk factors, BMI, and statin use). All continuous variables were standardized around the mean and presented as a Z-score. Abbreviations: HGU-hepatic glucose uptake, HAI-hepatic attenuation index, NAFLD-nonalcoholic fatty liver disease, MASLD-metabolic dysfunction associated steatotic liver disease, BM-bone marrow, CI-confidence interval. Grey shading of the blue fit line represents the 95 % confidence interval. (For interpretation of the references to color in this figure legend, the reader is referred to the web version of this article.)

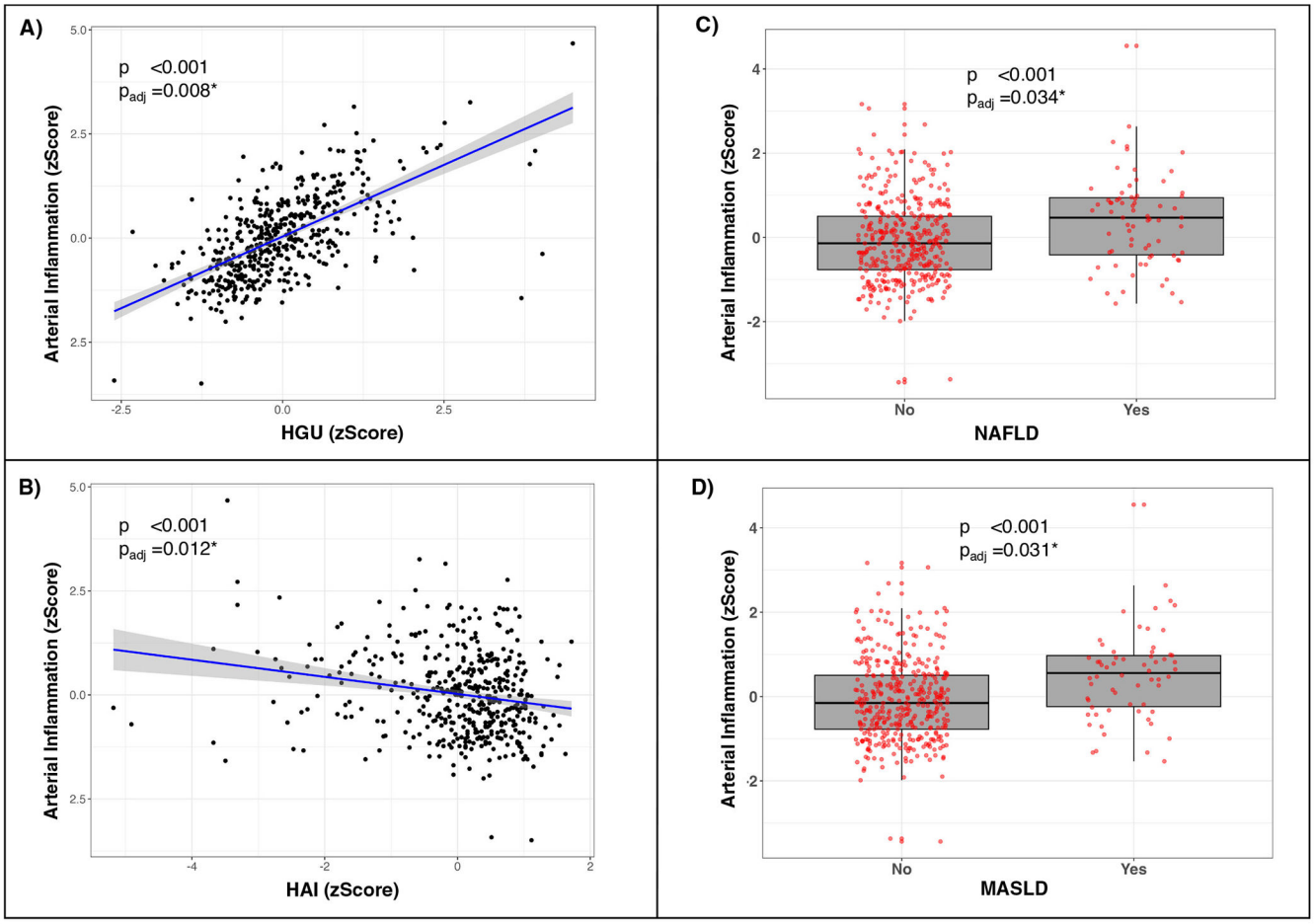

Fig. 3.

Association between imaging markers of hepatic steatosis and arterial inflammation among the entire cohort. * Adjusted for primary model (CVD risk factors, body mass index, and statin use). All continuous variables were standardized around the mean and presented as a Z-score. Abbreviations: HGU-hepatic glucose uptake, HAI-hepatic attenuation index, NAFLD-nonalcoholic fatty liver disease, MASLD-metabolic dysfunction associated steatotic liver disease, CI-confidence interval. Grey shading of the blue fit line represents the 95 % confidence interval. (For interpretation of the references to color in this figure legend, the reader is referred to the web version of this article.)

A: Multivariable Cox regression model

Model predictors	Multivariable Models	5-year MACE Risk		10-year MACE Risk	
		Cox Regression Model			
		Standardized HR (95% CI)	p-value	Standardized HR (95% CI)	p-value
Hepatic Glucose Uptake	A	1.491 (1.082, 2.054)	**0.015**	1.436 (1.146, 1.800)	**0.002**
	B	1.516 (1.101, 2.086)	**0.011**	1.370 (1.065, 1.761)	**0.014**
	C	1.503 (1.014, 2.226)	**0.042**	1.460 (1.107, 1.925)	**0.007**
	D	1.577 (1.142, 2.178)	**0.006**	1.357 (1.072, 1.716)	**0.011**
	E	1.518 (1.071, 2.151)	**0.019**	1.430 (1.080, 1.892)	**0.012**

Model A: univariable
Model B (primary): adjusted for CVD risk factors (i.e., age, sex, current smoking, diabetes mellitus, hyperlipidemia, hypertension), BMI, and statin use.
Model C: age, sex, and VAT/SAT ratio.
Model D: age, sex, and history of malignancy and chemotherapy/radiation.
Model E: age, sex, current smoking, diabetes mellitus, hyperlipidemia, hypertension, VAT/SAT ratio, statin use and history of malignancy history or chemotherapy/radiation.
Abbreviations: MACE- major adverse cardiovascular events, HR-hazard ratio, CI-confidence interval. Continuous variables were standardized.

B: Kaplan-Meier free survival curve of 10-year MACE risk.

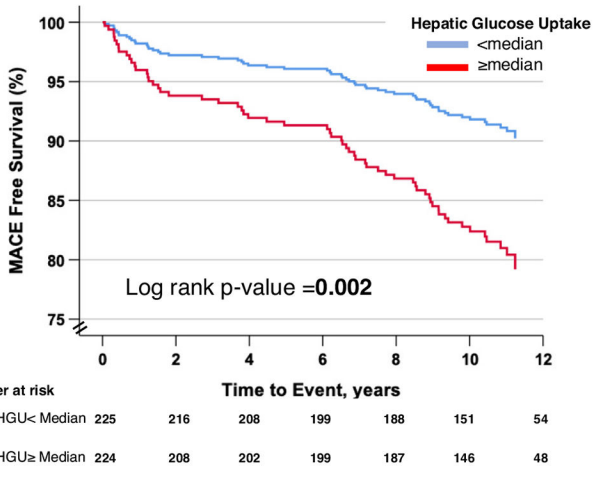

Fig. 4.

Associations between hepatic glucose uptake and MACE in the overall study cohort. A: Results of multivariable Cox regression models to assess 5-year and 10-year MACE risk, B: Kaplan Meier Survival Curve for individuals with (≥ vs. < population median) of HGU. The log-rank p-value is shown. Model A: univariable. Model B (primary): adjusted for CVD risk factors (i.e., age, sex, current smoking, diabetes mellitus, hyperlipidemia, hypertension), body mass index, and statin use. Model C: age, sex, and VAT/SAT ratio. Model D: age, sex, and malignancy history and treatment. Model E: age, sex, current smoking, diabetes mellitus, hyperlipidemia, hypertension, VAT/SAT ratio, statin use and history of malignancy history or chemotherapy/radiation. All continuous variables were standardized around the mean and presented as a Z-score. Abbreviations: HGU-hepatic glucose uptake; VAT/SAT-visceral adipose tissue/subcutaneous adipose tissue; MACE-major adverse cardiovascular events; HR-hazard ratio, CI-confidence interval.

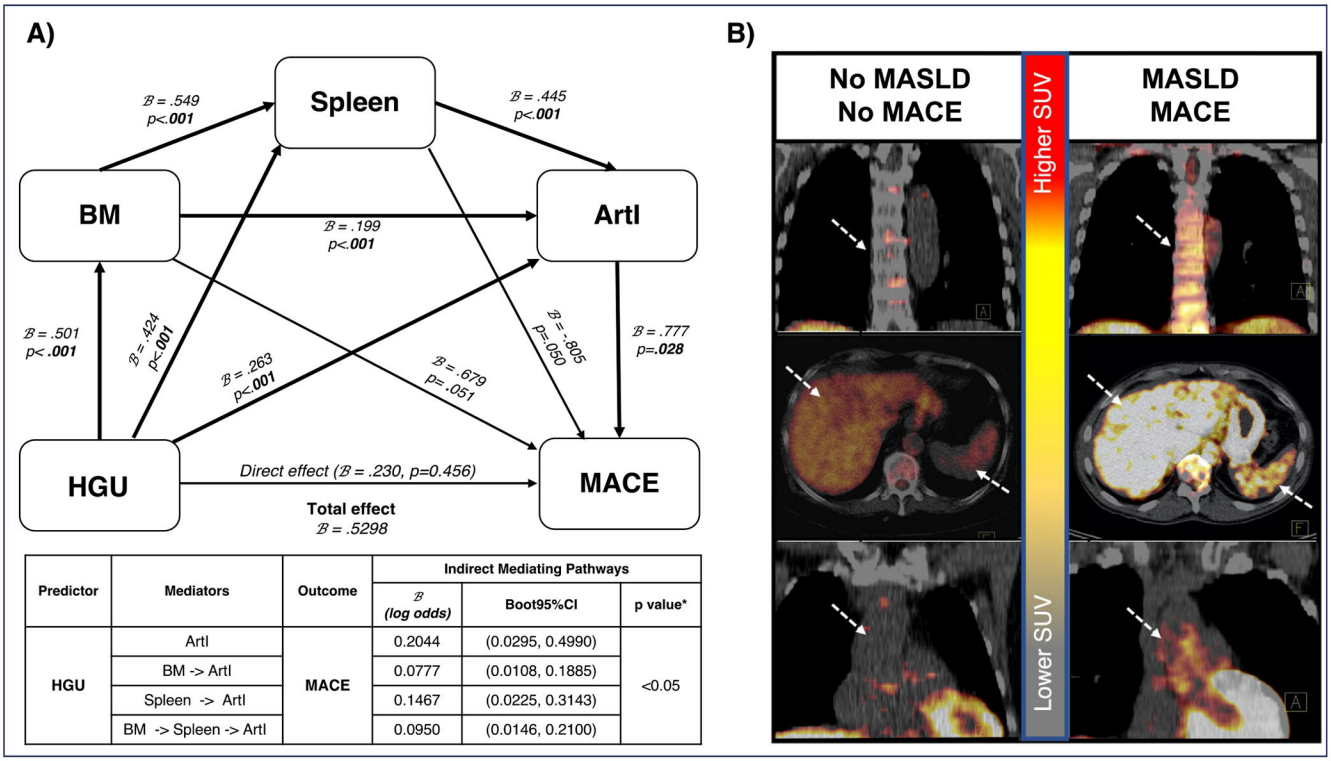

Predictor	Mediators	Outcome	Indirect Mediating Pathways		
			ℬ (log odds)	Boot95%CI	p value*
HGU	ArtI	MACE	0.2044	(0.0295, 0.4990)	<0.05
	BM -> ArtI		0.0777	(0.0108, 0.1885)	
	Spleen -> ArtI		0.1467	(0.0225, 0.3143)	
	BM -> Spleen -> ArtI		0.0950	(0.0146, 0.2100)	

Fig. 5.

A) Mediation analysis for the hypothesized pathways linking HGU and 5-year MACE in the entire cohort. Beta coefficients represent log odds. Continuous variables were standardized around the mean and are presented as a Z-score. *Models were adjusted for age and sex. Bootstrapping was utilized to generate 95 % CI for the log odds of indirect pathways, wherein statistical significance ($p < 0.05$) is indicated when 95 % CI not crossing zero. B) Example images of tissue activities on ^{18}F-FDG-PET/CT by MASLD status. Axial views of the spleen and liver (middle) and coronal views of the bone marrow (top) and aorta (bottom) are shown. Dotted white arrows refer to the activity in the respective tissue. Heightened tissue ^{18}F-FDG uptake is observed in an individual with MASLD and 5-year MACE (right) versus an individual without MASLD and no 5-year MACE (left). Abbreviations: MACE-major adverse cardiovascular event, MASLD-metabolic dysfunction associated steatotic liver disease, HGU-hepatic glucose uptake, ArtI-arterial inflammation, BM-bone marrow, SUV-standardized uptake value, ^{18}F-FDG-fluorodeoxyglucose, BootCI-confidence intervals calculated using bootstrapping.

Table 1

Baseline characteristics:

Characteristics	Full cohort (*n* = 445)	MASLD (*n* = 67)	No MASLD (*n* = 378)	p-Value
Age (years), median (IQR)	55 (44, 66)	57 (50, 68)	54.5 (44, 66)	**0.041**
Male, n (%)	194 (43.6)	36 (53.7)	158 (41.8)	**0.047**
Current smoker, n (%)	45 (10.2)	8 (11.9)	37 (9.9)	0.610
Diabetes mellitus (DM), n (%)	40 (9.0)	10 (14.9)	30 (8.0)	0.066
DM medications among diabetic individuals, n (%)				
None	13 (32.5)	4 (40)	9 (30)	0.305
Oral	21 (52.5)	6 (60)	15 (50)	
Insulin	6 (15)	–	6 (20)	
Prediabetes, n (%)	119 (26.7)	22 (32.8)	97 (25.7)	0.221
Hyperlipidemia, n (%)	122 (27.5)	27 (40.3)	95 (25.2)	**0.011**
Hypertension, n (%)	150 (33.8)	32 (47.8)	118 (31.3)	**0.007**
BMI [kg/m^2], n (%)				
<18.5	4 (0.9)	0 (0)	4 (1.1)	**<0.001**
18.5–25	164 (37.3)	5 (7.6)	159 (42.5)	
25–30	139 (31.6)	19 (28.8)	120 (32.1)	
≥30	133 (30.2)	42 (63.6)	91 (24.3)	
Statin use, n (%)	87 (19.6)	13 (19.4)	74 (19.6)	0.559
VAT volume (cm3), median (IQR)	48.5 (29.5, 75.2)	94 (67.2, 126.5)	44.9 (26.3, 63.6)	**<0.001**
SAT volume (cm3), median (IQR)	92.7 (65.1, 139)	124 (104, 173.8)	86.6 (60.6, 131.5)	**<0.001**
VAT/SAT Ratio, median (IQR)	0.52 (0.33, 0.75)	0.67 (0.53, 0.93)	0.49 (0.31, 0.71)	**<0.001**
Total Cholesterol [mg/dl], mean (SD)[a]	191 (44.1)	202 (44.2)	188.9 (43.9)	0.115
LDL [mg/dl], mean (SD)[a]	110 (38.0)	117.5 (33.7)	108.6 (38.6)	0.216
HDL [mg/dl], median (IQR)[a]	53 (43, 66)	45 (38, 57)	55.5 (44, 70)	**0.011**
Triglycerides [mg/dl], median (IQR)[a]	103 (74, 157)	163 (114.8, 202.5)	95 (72.3, 141)	**<0.001**
History of malignancy, n (%)	381 (85.6)	57 (85.1)	324 (85.7)	0.891
History of chemotherapy or radiation, n (%)	347 (78.0)	48 (71.6)	299 (79.1)	0.175
NAFLD, n (%)	70 (100)	67 (100)	3 (0.8)	**<0.001**

Data presented as median (IQR), mean (SD), or N (%), as appropriate. Abbreviations: NAFLD-nonalcoholic fatty liver disease, MASLD-Metabolic Dysfunction Associated Steatotic Liver disease, SD-standard deviation, IQR-interquartile range [25th, 75th], BMI-body mass index, VAT-visceral adipose tissue, SAT-subcutaneous adipose tissue, ^{18}F-FDG-^{18}F-Fluorodeoxyglucose, LDL-low density lipoprotein, HDL-high density lipoprotein. Bold values indicate statistical significance ($p < 0.05$).

[a]Data were available for only 218 subjects.

Table 2

Multivariable Associations between hepatic steatosis and leukopoietic tissue activities and arterial inflammation in overall study cohort.

Model predictors	Multivariable models	Tissue activities					
		Arterial inflammation		Bone marrow activity		Splenic activity	
		Standardized β (95 % CI)	p-Value	Standardized β (95 % CI)	p-Value	Standardized β (95 % CI)	p-Value
Hepatic Glucose Uptake	A	0.578 (0.501, 0.655)	**<0.001**	0.377 (0.300, 0.454)	**<0.001**	0.594 (0.522, 0.666)	**<0.001**
	B	0.529 (0.453, 0.605)	**<0.001**	0.353 (0.276, 0.430)	**<0.001**	0.548 (0.475, 0.621)	**<0.001**
	C	0.537 (0.457, 0.617)	**<0.001**	0.341 (0.259, 0.423)	**<0.001**	0.519 (0.444, 0.595)	**<0.001**
	D	0.568 (0.492, 0.643)	**<0.001**	0.387 (0.310, 0.463)	**<0.001**	0.585 (0.512, 0.658)	**<0.001**
	E	0.629 (0.541, 0.716)	**<0.001**	0.451 (0.362, 0.539)	**<0.001**	0.621 (0.541, 0.702)	**<0.001**
Hepatic Attenuation Index	A	−0.206 (−0.300, −0.112)	**<0.001**	−0.252 (−0.337, −0.167)	**<0.001**	−0.291 (−0.381, −0.202)	**<0.001**
	B	−0.116 (−0.207, −0.025)	**0.012**	−0.186 (−0.271, −0.101)	**<0.001**	−0.204 (−0.294, −0.114)	**<0.001**
	C	−0.139 (−0.242, −0.035)	**0.009**	−0.197 (−0.291, −0.103)	**<0.001**	−0.210 (−0.306, −0.115)	**<0.001**
	D	−0.171 (−0.263, −0.080)	**<0.001**	−0.236 (−0.319, −0.153)	**<0.001**	−0.267 (−0.356, −0.179)	**<0.001**
	E	−0.105 (−0.209, −0.001)	**0.048**	−0.173 (−0.269, −0.077)	**<0.001**	−0.181 (−0.279, −0.083)	**<0.001**
NAFLD	A	0.490 (0.232, 0.748)	**<0.001**	0.455 (0.218, 0.692)	**<0.001**	0.698 (0.450, 0.945)	**<0.001**
	B	0.270 (0.020, 0.520)	**0.034**	0.341 (0.108, 0.574)	**0.004**	0.478 (0.230, 0.725)	**<0.001**
	C	0.435 (0.161, 0.709)	**0.002**	0.377 (0.124, 0.630)	**0.004**	0.524 (0.270, 0.778)	**<0.001**
	D	0.424 (0.171, 0.671)	**0.001**	0.440 (0.205, 0.674)	**<0.001**	0.642 (0.396, 0.888)	**<0.001**
	E	0.371 (0.093, 0.648)	**0.009**	0.327 (0.072, 0.582)	**0.012**	0.485 (0.229, 0.741)	**<0.001**
MASLD	A	0.619 (0.358, 0.880)	**<0.001**	0.534 (0.264, 0.804)	**<0.001**	0.809 (0.545, 1.073)	**<0.001**
	B	0.291 (0.026, 0.556)	**0.031**	0.349 (0.076, 0.623)	**0.012**	0.491 (0.210, 0.772)	**<0.001**
	C	0.571 (0.288, 0.854)	**<0.001**	0.484 (0.218, 0.750)	**<0.001**	0.626 (0.353, 0.898)	**<0.001**
	D	0.549 (0.293, 0.804)	**<0.001**	0.530 (0.261, 0.799)	**<0.001**	0.761 (0.497, 1.026)	**<0.001**
	E	0.366 (0.080, 0.651)	**0.012**	0.343 (0.081, 0.604)	**0.010**	0.497 (0.233, 0.761)	**<0.001**

Model A: univariable.

Model B (primary): adjusted for cardiovascular disease risk factors (i.e., age, sex, current smoking, diabetes mellitus, hyperlipidemia, hypertension), body mass index, and statin use.

Model C: age, sex, and VAT/SAT ratio.

Model D: Age, sex, and history of malignancy history or chemotherapy/radiation.

Model E: adjusted for cardiovascular disease risk factors (i.e., age, sex, current smoking, diabetes mellitus, hyperlipidemia, hypertension), VAT/SAT ratio, statin use and history of malignancy history or chemotherapy/radiation.

Abbreviations: NAFLD-nonalcoholic fatty liver disease, MASLD-metabolic dysfunction associated steatotic liver disease, VAT-visceral adipose tissue, SAT-subcutaneous adipose tissue, CI-confidence interval. All continuous variables were standardized around the mean and presented as a *Z*-score.

Bold values indicate statistical significance ($p < 0.05$).